

## The Sloan Digital Sky Survey Quasar Lens Search. IV. Statistical Lens Sample from the Fifth Data Release

Naohisa Inada,<sup>1,2</sup> Masamune Oguri,<sup>3,4</sup> Min-Su Shin,<sup>5,6</sup> Issha Kayo,<sup>7,8</sup> Michael A. Strauss,<sup>6</sup>  
Joseph F. Hennawi,<sup>9,10</sup> Tomoki Morokuma,<sup>8,11</sup> Robert H. Becker,<sup>12,13</sup> Richard L. White,<sup>14</sup>  
Christopher S. Kochanek,<sup>15</sup> Michael D. Gregg,<sup>12,13</sup> Kuenley Chiu,<sup>16</sup> David E. Johnston,<sup>17</sup>  
Alejandro Clocchiatti,<sup>18</sup> Gordon T. Richards,<sup>19</sup> Donald P. Schneider,<sup>20</sup> Joshua A.  
Frieman,<sup>21,22,23</sup> Masataka Fukugita,<sup>7,24,25</sup> J. Richard Gott, III,<sup>6</sup> Patrick B. Hall,<sup>26</sup> Donald  
G. York,<sup>23,27</sup> Francisco J. Castander,<sup>28</sup> and Neta A. Bahcall<sup>6</sup>

---

<sup>1</sup>Cosmic Radiation Laboratory, RIKEN, 2-1 Hirosawa, Wako, Saitama 351-0198, Japan.

<sup>2</sup>Research Center for the Early Universe, School of Science, University of Tokyo, Bunkyo-ku, Tokyo 113-0033, Japan.

<sup>3</sup>Division of Theoretical Astronomy, National Astronomical Observatory, 2-21-1, Osawa, Mitaka, Tokyo 181-8588, Japan.

<sup>4</sup>Kavli Institute for Particle Astrophysics and Cosmology, Stanford University, 2575 Sand Hill Road, Menlo Park, CA 94025, USA.

<sup>5</sup>Department of Astronomy, University of Michigan, 500 Church Street, Ann Arbor, MI 48109-1042 USA.

<sup>6</sup>Princeton University Observatory, Peyton Hall, Princeton, NJ 08544, USA.

<sup>7</sup>Institute of the Physics and Mathematics of the Universe, University of Tokyo, Kashiwa, 277-8582, Japan.

<sup>8</sup>Research Fellow of the Japan Society for the Promotion of Science.

<sup>9</sup>Department of Astronomy, University of California Berkeley, 601 Campbell Hall, Berkeley, CA 94720-3411, USA.

<sup>10</sup>Max Planck Institut für Astronomie, Königstuhl 17, 69117 Heidelberg, Germany.

<sup>11</sup>Optical and Infrared Astronomy Division, National Astronomical Observatory, 2-21-1 Osawa, Mitaka, Tokyo 181-8588, Japan.

<sup>12</sup>IGPP-LLNL, L-413, 7000 East Avenue, Livermore, CA 94550, USA.

<sup>13</sup>Department of Physics, University of California Davis, 1 Shields Avenue, Davis, CA 95616, USA.

<sup>14</sup>Space Telescope Science Institute, 3700 San Martin Drive, Baltimore, MD 21218, USA.

<sup>15</sup>Department of Astronomy, The Ohio State University, Columbus, OH 43210, USA.

<sup>16</sup>School of Physics, University of Exeter, Stocker Road, Exeter EX4 4QL, UK.

<sup>17</sup>Jet Propulsion Laboratory, 4800 Oak Grove Drive, Pasadena CA, 91109, USA.

<sup>18</sup>Departamento de Astronomía y Astrofísica, Pontificia Universidad Católica de Chile, Casilla 306, Santiago 22, Chile.

<sup>19</sup>Department of Physics, Drexel University, 3141 Chestnut Street, Philadelphia, PA 19104, USA.

<sup>20</sup>Department of Astronomy and Astrophysics, The Pennsylvania State University, 525 Davey Laboratory, University Park, PA 16802, USA.

<sup>21</sup>Kavli Institute for Cosmological Physics, University of Chicago, Chicago, IL 60637, USA.

<sup>22</sup>Center for Particle Astrophysics, Fermi National Accelerator Laboratory, P.O. Box 500, Batavia, IL 60510, USA.

<sup>23</sup>Department of Astronomy and Astrophysics, The University of Chicago, 5640 South Ellis Avenue, Chicago, IL 60637, USA.

## ABSTRACT

We present the second report of our systematic search for strongly lensed quasars from the data of the Sloan Digital Sky Survey (SDSS). From extensive follow-up observations of 136 candidate objects, we find 36 lenses in the full sample of 77,429 spectroscopically confirmed quasars in the SDSS Data Release 5. We then define a complete sample of 19 lenses, including 11 from our previous search in the SDSS Data Release 3, from the sample of 36,287 quasars with  $i < 19.1$  in the redshift range  $0.6 < z < 2.2$ , where we require the lenses to have image separations of  $1'' < \theta < 20''$  and  $i$ -band magnitude differences between the two images smaller than 1.25 mag. Among the 19 lensed quasars, 3 have quadruple-image configurations, while the remaining 16 show double images. This lens sample constrains the cosmological constant to be  $\Omega_\Lambda = 0.84_{-0.08}^{+0.06}(\text{stat.})_{-0.07}^{+0.09}(\text{syst.})$  assuming a flat universe, which is in good agreement with other cosmological observations. We also report the discoveries of 7 binary quasars with separations ranging from  $1''.1$  to  $16''.6$ , which are identified in the course of our lens survey. This study concludes the construction of our statistical lens sample in the full SDSS-I data set.

*Subject headings:* gravitational lensing: strong — quasars: general — cosmology: observations

## 1. INTRODUCTION

Gravitationally lensed quasars are useful tools for a variety of astrophysical and cosmological studies (e.g., Turner et al. 1984; Blandford & Kochanek 1987; Schneider et al. 1992; Kochanek et al. 2006). In particular, statistical analyses of lensed quasars serve as a useful probe for the cosmological constant (Fukugita et al. 1990; Turner 1990) and the Hubble constant (Oguri 2007a). The Hubble Space Telescope (*HST*) Snapshot survey (Maoz et al.

---

<sup>24</sup>Institute for Cosmic Ray Research, University of Tokyo, Kashiwa, 277-8582, Japan.

<sup>25</sup>Institute for Advanced Study, Princeton, NJ08540, USA.

<sup>26</sup>Department of Physics and Astronomy, York University, 4700 Keele Street, Toronto, Ontario, M3J 1P3, Canada.

<sup>27</sup>Enrico Fermi Institute, The University of Chicago, 5640 South Ellis Avenue, Chicago, IL 60637, USA.

<sup>28</sup>Institut de Ciències de l'Espai (IEEC/CSIC), Campus UAB, 08193 Bellaterra, Barcelona, Spain.

1993) and the Cosmic-Lens All Sky Survey (CLASS; Myers et al. 2003; Browne et al. 2003) have provided examples of complete lens samples that have allowed cosmological studies. The *HST* Snapshot survey includes five lenses selected from 502 bright, relatively high-redshift quasars, and was used to derive a limit on the cosmological constant (Maoz et al. 1993). It was also used to study galaxy evolution by combining with other lens surveys (Chae 2010). CLASS contains 13 lenses from 8958 radio sources; the redshift distribution of this sample is not well determined (e.g., Muñoz et al. 2003). This sample has also been used to constrain cosmological models as well as the structure and evolution of lens galaxies (e.g., Rusin & Tegmark 2001; Mitchell et al. 2005; Chae et al. 2006). While large samples of galaxy-galaxy lenses are being assembled by various groups (e.g., Bolton et al. 2006, 2008; Cabanac et al. 2007; Faure et al. 2008; Marshall et al. 2009; Kubo et al. 2009; Féron et al. 2009) and are used to study the structure of the lens galaxies, they are not well suited as a cosmological probe because galaxy-galaxy lenses are often selected from samples of lensing objects, not source objects, much complicating the statistics.

In order to construct a large statistical sample of lensed quasars that can be used as a cosmological probe, we have conducted the Sloan Digital Sky Survey Quasar Lens Search (SQLS; Oguri et al. 2006, hereafter Paper I) based on a sample of spectroscopically confirmed quasars (Schneider et al. 2007) derived from the Sloan Digital Sky Survey (SDSS; York et al. 2000). To allow cosmological tests, the lens sample must be complete with well-defined criteria. We refer to a sample that allows statistical tests as a “statistical sample”. Our lens sample is, in fact, designed to be complete under prescribed conditions and therefore suitable for statistical studies and cosmological tests, given the accurately defined selection function (see Paper I) and the homogeneity of the SDSS data. In Inada et al. (2008), hereafter Paper II, we presented a complete sample of 11 lensed quasars suitable for statistical analyses, selected from the 22,683 quasars satisfying  $0.6 < z < 2.2$  and  $i < 19.1^1$  out of the total of 46,420 quasars (Schneider et al. 2005) in the SDSS Data Release 3 (DR3; Abazajian et al. 2005). This sample derived from the DR3 gives cosmological constraints (Oguri et al. 2008a, hereafter Paper III) that agree with the current cosmological model (e.g., Komatsu et al. 2009; Tegmark et al. 2006).

In this paper, we extend our source population to the SDSS Data Release 5 (DR5; Adelman-McCarthy 2007), concluding the SDSS-I (the first phase of the SDSS project through 2005 June). The selection process is the same as that used to create the DR3 statistical sample of lenses, as described in Paper II. Note that all lensed quasars described in this paper have already been reported in their discovery papers. The main focus of this

---

<sup>1</sup>Here  $i$  is the Point Spread Function (PSF) magnitude corrected for Galactic extinction from the maps of Schlegel et al. (1998).

paper is to define the DR5 statistical sample, and to report quasars that turned out not to be gravitational lenses. We briefly describe the source quasar sample from which we constructed the DR5 statistical lens sample in Section 2, and the selection of lens candidates in Section 3. We present observational results for the lensing candidates in Section 4, and the resulting DR5 lensed quasar sample and updates of cosmological constraints in Section 5. Section 6 gives a summary of our results.

## 2. SOURCE QUASARS

The SDSS is a combination of photometric and spectroscopic surveys of a quarter of the sky, primarily in a region centered on the North Galactic Cap. The surveys were carried out using a dedicated wide-field 2.5-m telescope (Gunn et al. 2006) at the Apache Point Observatory in New Mexico, USA. The details of the photometric survey using five broad-band optical filters (*ugriz*), including the astrometric accuracy and photometric zero point accuracy, are described in Fukugita et al. (1996), Gunn et al. (1998), Hogg et al. (2001), Smith et al. (2002), Pier et al. (2003), Ivezić et al. (2004), Tucker et al. (2006), and Padmanabhan et al. (2008). The data of the photometric survey are processed by the photometric pipeline (Lupton et al. 2001). The target selection pipeline (Richards et al. 2002) finds quasar candidates for the spectroscopic survey. The candidates are tiled on each plate according to the algorithm of Blanton et al. (2003). Spectroscopic observations with a resolution of  $R \sim 1800$  are carried out using a pair of multi-fiber double spectrographs covering 3800 Å to 9200 Å. The SDSS data have been published in series of Data Releases (Stoughton et al. 2002; Abazajian et al. 2003, 2004, 2005, 2009; Adelman-McCarthy 2006, 2007).

We construct a source quasar sample following the procedure in Paper II. We start with the 77,429 quasars in the DR5 spectroscopic survey selected over an area of 5740 deg<sup>2</sup> (Schneider et al. 2007), and restrict the redshift range to  $0.6 < z < 2.2$  and magnitude to  $i < 19.1$ , over which the quasar target selection is almost complete (see Paper I) and does not significantly bias our lens candidate search. The lower redshift limit is imposed to eliminate quasars associated with resolved host galaxies, which otherwise would dominate our candidate list, based in part on the extent of the optical image. We further exclude quasars in poor seeing fields,  $\text{PSF\_WIDTH} > 1''.8$ , where identification of close pairs becomes difficult. These selection criteria give a sample of 36,287 quasars<sup>2</sup>. Removing DR3 quasars

---

<sup>2</sup>See the SQLS webpage (<http://www-utap.phys.s.u-tokyo.ac.jp/~sdss/sqls/>) for the list of the 36,287 quasars.

that have already been studied in Paper II, we are left with 13,636 quasars<sup>3</sup> to be studied in this work.

### 3. LENS CANDIDATES

Our SQLS selection procedure to identify lensed quasar candidates uses two different algorithms; “morphological selection” to find small separation lensed quasars ( $\theta \lesssim 2''.5$ ) which are not deblended into multiple components by the SDSS photometric pipeline, and “color selection” to find large separation lenses ( $\theta \gtrsim 2''.5$ ) whose lensed components are deblended and thus registered as separate objects in the SDSS image catalog.

In brief, morphological selection finds quasars that appear as single objects but are not well fit with the PSF. This is represented by the parameter `star_L` for each color band which gives the logarithmic likelihood that the object is fit by the PSF. The values used in the `star_L` cut (see Paper II) were tested against many simulated lensed quasars, as described in Paper I. We then fit each system to a model with two PSFs using GALFIT (Peng et al. 2002), to exclude objects that are single quasars, or obvious quasar-star or -galaxy associations. If these objects are fit with two PSFs, the GALFIT for single filter images results in either very small separations of the two centroids, or very large magnitude differences in the two components: with data in several bands, the two decomposed objects may become mutually inconsistent for their positions and/or colors. Therefore, we can select lens candidates by choosing objects whose  $u$ - and  $i$ -band image fits are both “normal” and are in good positional agreement (see, more quantitatively, Equation 16 of Paper I). In practice, it is sufficient to use the  $u$ -band and one of the  $gri$ -band images for objects at  $z < 2.2$ . The candidates which survive the GALFIT selection are visually inspected to exclude objects that are clearly superpositions of a quasar and a galaxy, particularly using their bluer band images where signals from quasar components ( $z < 2.2$ ) are much more dominant than those from galaxies. Of the 13,636 quasars, 50 morphologically-selected candidates survive this selection. This selection is designed to pick up all lenses that satisfy the relative brightness criterion ( $|\Delta i| < 1.25$ ; see below) with separations between  $1''$  and  $2''$ . The 50 candidates we obtained are listed in Table 2.

The color selection algorithm applies to the case where the lensed images are deblended by the photometric pipeline. We search for objects around each quasar having colors similar

---

<sup>3</sup>The number of DR3 quasars in this paper (22,651) differs slightly from that given in Paper II (22,683). 32 quasars in the DR3 are given different parameters (magnitudes) in the DR5 catalog and no longer meet the criteria for our source sample. This does not affect the number of lenses or lens candidates in the DR3.

to those of the quasar. To obtain a complete sample with image separations  $1'' < \theta < 20''$  and  $i$ -band magnitude differences between two images  $|\Delta i| < 1.25$ , we search for objects with  $\theta < 20''.1$  and  $|\Delta i| < 1.3$  allowing for some tolerance. Next we exclude some candidates whose optical and radio flux ratios are inconsistent between the two components (Kochanek et al. 1999). We used the data from the Faint Images of the Radio Sky at Twenty centimeters survey (FIRST; Becker et al. 1995) for candidates with image separations larger than  $6''$ , which is the resolution of FIRST. We also reject some obvious quasar-galaxy pairs by visual inspection. We exclude low-redshift and large-separation pairs with no detectable lensing objects in the SDSS image, because a standard galaxy model predicts that at least one of the member galaxies of the putative lens group/cluster should be detectable for such lens events (see Paper II for quantitative details). We consider all lens candidates with separations larger than the minimum deblending separation ( $\sim 1''.5$ ) of the SDSS photometric pipeline, amounting to 88 candidates from the 13,636 quasars. Two objects out of the 88 candidates are selected by both the morphological and color selection algorithms, and therefore 86 candidates are listed in Table 3. The numbers of objects selected by the two algorithms are summarized in Table 1.

## 4. OBSERVATIONS

### 4.1. Summary of Follow-up Observations

The 136 lensed quasar candidates taken from the 13,636 quasars constitute our targets for follow-up observations, but we remove two candidates that have already been examined. One is the morphologically selected candidate SDSS J111816.95+074558.1 which is the well-known lensed quasar PG1115+080 (Weymann et al. 1980). The other is the color selected candidate SDSS J165502.02+260516.5, which is a pair of quasars with slightly different redshifts from SDSS spectroscopy. The remaining 134 candidates were observed as described in what follows using various telescopic facilities. The observations include optical and/or near-infrared imaging and optical spectroscopy, and are tabulated in Table 2 and Table 3.

For the 49 morphologically-selected candidates after excluding SDSS J111816.95+074558.1, we first carry out optical ( $i$  or  $I$ ) and/or infrared ( $H$ ,  $K$ , or  $K'$ ) imaging under good seeing conditions ( $\sim 0''.5 - 1''.0$ ) to confirm that the candidates indeed have two or more stellar components and also a lens galaxy between the stellar components. We set the exposure time such that we can detect faint extended objects down to  $I \sim 23.0$ ,  $H \sim 18.5$ , and  $K \sim 20.0$  at  $S/N \simeq 10$ , corresponding to the brightness at which one can detect lens galaxies if they are located at a redshift half that of the source quasar. Figure 1 shows the relation between the image separation and the rest-frame  $I$  (or  $i$ ) band luminosity of the lens galaxies. The

13 filled circles are the luminosities of the lens galaxies that are included in our statistical sample and have measured redshifts (see Table 4). Open circles are upper limit on the luminosities of hypothetical lens galaxies of the candidates with “no lens object” (but not “binary QSO”) in Table 2 or Table 3, assuming that the lens galaxy is located at half the source redshift. The assumption is reasonable given that the maximum value of the ratio of lens to source redshifts  $z_l/z_s$  in our statistical sample is 0.60, and that 90% of the lens galaxies are located at  $z_l/z_s < 0.5$ . Open triangles refer to binary quasars which we discuss at length in Section 4.2, where a more extreme lens redshift  $z_l = z_s$  is assumed. The figure indicates that the luminosities of candidate lens galaxies with no detection are significantly fainter than what would be expected for a given separation angle expected from our confirmed lensing events. This is particularly true if we consider the fact that a positive correlation is expected between luminosity and the separation angle, as simple lens models predict. The empirical correlation between the mass and luminosity of early-type galaxies also predicts the minimum apparent luminosities of lens galaxies (e.g., Rusin et al. 2003), and our detection limit corresponds to luminosities typically much fainter than this predicted minimum. For this reason we exclude as lensing candidates those cases which do not exhibit any signatures of lens galaxy in our follow-up images. However, we obtained follow-up spectroscopy for four candidates which were judged to be particularly good candidates based on the color and morphology of their SDSS images, even though our follow-up images for these candidates show no sign of lensing objects.

Some candidates were rejected because they turn out to be single quasars or quasar-galaxy associations. For candidates that are not excluded at this step, we acquire spectra of the stellar components. Of the seven targets with possible lensing objects, five of them are lensed quasars (six in the list of morphologically selected systems when PG1115+080 is included). The other two objects were found to be binary quasars (see Section 4.2). The four additional spectroscopic targets described above were found not to be lensed quasars.

For the 85 color-selected candidates (after excluding SDSS J165502.02+260516.5), we carry out either optical/near-infrared imaging or optical spectroscopy of the stellar components. For imaging we first looked for archival data from the Subaru telescope (SMOKA; Baba et al. 2002), and found that SDSS J134150.74+283207.9 could be rejected due to the absence of any possible lensing objects in the deep Subaru image. Follow-up imaging of 50 candidates yields five cases that indicate signatures of possible lens galaxies. Subsequent spectroscopy of these five objects shows that four of them are lensed quasars, and the remaining one, SDSS J160614.69+230518.0, is a quasar-star pair. We carried out spectroscopy of the remaining 34 candidates without imaging, which yielded five pairs of quasars with the same redshifts. Two of the five were found not to be lensed quasars because they have different spectral energy distributions not consistent with being lensed pairs. The other



three pairs were also rejected due to the lack of lensing objects in deep follow-up images (see Section 4.2). We also carried out additional spectroscopy for four objects that did not show a lensing object in the images, but which look visually like promising lens candidates. We confirmed, however, that they each are a quasar-star pair. In conclusion we found four lensed quasars among the color-selected candidates.

We remark that our selection process would reject “dark lenses”, in which the mass-to-light ratio of the lens galaxy is unusually large. The possibility of dark lenses has been discussed in, e.g., Rusin (2002) and Ryan et al. (2008), although there are no unambiguous cases of such dark lenses in the literature.

## 4.2. Newly Discovered Binary Quasars

We found 29 objects that have multiple quasar components among the 136 candidates. Ten of them are lensed quasars, and four of them are known pairs of quasars with different redshifts reported in Hennawi et al. (2006a). Eight systems are pairs of quasars, which we found to have different redshifts. The remaining seven systems consist of quasar pairs with identical redshifts. We, however, do not consider them to be lenses, for the reasons we discuss in what follows.

**SDSS J101211.29+365030.7:** We detect C IV ( $\sim 4130\text{\AA}$ ) and C III] ( $\sim 5100\text{\AA}$ ) emission lines at  $z = 1.678$  in both of the components separated by  $16''.6$ , in follow-up spectroscopy at the ARC 3.5-m telescope. Deep optical and near-infrared imaging with a detection limit ( $S/N \simeq 10$ ) corresponding to  $M_I \sim -21.3$  at  $z = 1.678$ , however, do not show a galaxy cluster between the two quasar images, which would be necessary to produce this large image separation. Therefore, this object, SDSS J1012+3650, is taken to be a binary quasar.

**SDSS J151109.85+335701.7:** The images of this candidate show two point sources separated by  $\theta = 1''.1$ . We detected a signature of a possible lens galaxy when we subtract two PSFs from the UH88  $I$ -band image. We then obtained spectra of the two stellar components and a deeper  $I$ -band image using the Subaru telescope under good seeing conditions ( $0''.6$ ). The C II and Mg II emission lines redshifted to  $z = 0.799$  have similar shapes in the two objects. The slopes of the continua are also similar. We do not find, however, a galaxy between the two quasars at a detection limit ( $S/N \simeq 10$ ) of  $M_I \sim -19.9$  (at  $z = 0.799$ ) in the Subaru image. This suggests that the residual flux arises from the host galaxies of the two quasars.

**SDSS J151823.05+295925.4:** We obtained spectra of the two components using the ARC 3.5-m telescope. The shapes of the C III] and Mg II emission lines at  $z = 1.249$  are

similar. However, we do not find any galaxies between the two quasars in a deep optical image taken at UH88 to a detection limit ( $S/N \simeq 10$ ) of  $M_i \sim -20.6$  at  $z = 1.249$ . Based on the lensing criteria described in Section 4.1, we conclude that SDSS J1518+2959 is a binary quasar with  $\theta = 5''.3$ .

**SDSS J155218.09+045635.2:** The spectra of the two components were obtained at the ARC 3.5-m telescope. While the brighter component has a clear Broad Absorption Line (BAL) feature in its C IV emission line at  $z = 1.567$ , the fainter one does not show a BAL feature. In addition, we do not detect any signature of a massive galaxy cluster in the deep UH88 *I*-band image, which would be necessary to account for the large image separation of  $\theta = 11''.7$ .

**SDSS J155225.62+300902.0:** This system was considered to be a promising morphologically-selected candidate, with a possible lens galaxy detected in UH88 *I*-band and UKIRT *K*-band images. We took spectra of the two stellar components ( $\theta = 1''.3$ ) using the Subaru telescope. Although the Mg II emission line of the fainter component at  $z = 0.750$  is slightly broader than that of the brighter component, the two quasars have similar continua. As in the case of SDSS J1511+3357, however, we find no galaxy between the two components at a detection limit ( $S/N \simeq 10$ ) of  $M_I \sim -19.8$  at  $z = 0.750$  in the deep *I*-band Subaru image (seeing  $\sim 0''.6$ ), except for extended residuals around the two quasars that represent the host galaxies of the quasars.

**SDSS J160602.81+290048.7:** The two stellar components separated by  $\theta = 3''.5$  have similar shapes for the Mg II emission lines at  $z = 0.770$  and the continua in our follow-up spectra taken at the ARC 3.5-m telescope. We do not find, however, a lens galaxy between the two quasar components at a detection limit ( $S/N \simeq 10$ ) of  $M_i \sim -19.3$  at  $z = 0.770$  in the deep *i*-band image with the ARC 3.5-m telescope.

**SDSS J163520.04+205225.1:** We obtained spectra of the two components ( $\theta = 13''.6$ ) at the TNG 3.6m telescope. The C IV emission lines at  $z = 1.775$  revealed that the fainter component is probably a BAL quasar whereas the brighter component is not. Along with the absence of a lens cluster of galaxies in deep images taken at the UH88 and KPNO 2.1m telescopes, we conclude that this object is a binary quasar.

To summarize, two (SDSS J1552+0456 and SDSS J1635+2052) of the seven candidates are found to be binary quasars from their different spectral energy distributions. The other five objects are also classified as binary quasars, based on the failure to detect lensing objects in our imaging follow-up observations, which were deep enough to detect galaxies down to magnitudes significantly fainter than those of lensing galaxies for our confirmed lens sample (see Figure 1).

## 5. IDENTIFIED LENSED QUASARS

### 5.1. Statistical Sample

We construct a DR5 complete sample of lensed quasars with image separations of  $1'' < \theta < 20''$  and absolute  $i$ -band (or  $I$ -band) magnitude differences less than 1.25 mag for doubles. We do not set any magnitude difference limits for quadruples. Simulations described in Paper I suggest that our lens selection is almost complete within these ranges. From the 13,636 quasars we selected 136 candidates for lensing, among which we confirmed ten lensed quasars, six based on morphological selection (including the known one, PG1115+080) and four based on color selection. Eight of the ten meet the criteria we set for the separation angle and the flux ratio, while SDSS J132236.41+105239.4 and SDSS J134929.84+122706.9 lie outside the criteria. Including the 11 lensed quasars from the DR3 sample (Paper II), our DR5 statistical sample consists of 19 lensed quasars selected from a sample of 36,287 quasars, as summarized in Table 4. The details of the 19 lensed quasars are given in the discovery papers cited in Table 4. We note that we recover all previously known lenses (CASTLES webpage<sup>4</sup>) that satisfy our criteria in the area of the DR5 spectroscopic survey.

Figure 2 shows the distribution of the image separations of the statistical sample. We obtain updated constraints on cosmological parameters by simply repeating the calculation done in Paper III, assuming a flat universe. The details of the calculation are given in Paper III; in brief, we compute the expected numbers of small-separation lensed quasars for different cosmological models, and compare them with our statistical lens sample in the image separation range of  $1'' < \theta < 3''$ . We consider lensing by single elliptical galaxies which are modeled by singular isothermal ellipsoids. We adopt the velocity function of Choi et al. (2007). The magnification bias is estimated (see Equations 6, 7, and 8 of Paper III) using the image separation-dependent magnification factor derived in Paper I and the quasar luminosity function obtained by Richards et al. (2005). As in Paper III, we require that the PSF magnitude of the quasar components must be brighter than the lens galaxy. Since our calculation takes only early-type galaxies into account, we remove SDSS J1313+5151 whose lens galaxy is fit by a Sérsic profile with  $n = 1$  (Ofek et al. 2007) and looks somewhat bluer, and hence is likely to be a late-type galaxy. From the subsample of 14 lenses, the cosmological constant is constrained to be  $\Omega_\Lambda = 0.84_{-0.08}^{+0.06}(\text{stat.})_{-0.07}^{+0.09}(\text{syst.})$ . A hypothetical case that we have 15 lenses in the subsample (we add one more lens with  $\theta \sim 1''.0$ ) increases the value of  $\Omega_\Lambda$  in  $\sim 0.02$ . The largest source of systematic errors is the uncertainties in the velocity function of the lens galaxies and its redshift evolution; see Table 2 and Section 4.3 of Paper

---

<sup>4</sup> <http://cfa-www.harvard.edu/castles/>.

III for comprehensive discussions of the systematic errors. If we account for the statistical error only, our result rejects  $\Omega_\Lambda = 0$  at the  $5\sigma$  level, as estimated from the full likelihood distribution. Next we allow the dark energy equation of state to vary, and derive constraints in the two-dimensional parameter space of  $\Omega_M$  and  $w$ . By combining our result with the results from the SDSS baryon acoustic oscillation measurements in the SDSS galaxy two-point correlation function (Eisenstein et al. 2005), we obtain  $\Omega_M = 0.23_{-0.03}^{+0.04}(\text{stat.})_{-0.04}^{+0.03}(\text{syst.})$  and  $w = -1.4 \pm 0.3(\text{stat.})_{-0.4}^{+0.3}(\text{syst.})$ .

The fraction of quadruple lenses in the DR5 statistical sample is 16% (see Table 4), which is lower than the fraction in the CLASS survey of 46%. This might be ascribed to the shallower slope of the luminosity function at the survey flux limit of SQLS than that at the CLASS limit (see, e.g., Oguri 2007b, for more detailed discussion).

## 5.2. Additional Lensed Quasars

We also searched for lensed quasars in the DR5 sample which do not satisfy the conditions,  $0.6 < z < 2.2$ ,  $i < 19.1$  and  $\text{PSF\_WIDTH} < 1''8$ , with the understanding that the resulting sample will not be complete. The candidate selection is somewhat extended from that used to make the statistical sample. For high redshift ( $z > 2.2$ ) quasars, for instance, we use the `star_L` criteria for the *griz* bands rather than the *ugri* bands (e.g., Inada et al. 2009). We discovered two lensed quasars, SDSS J0819+5356 (Inada et al. 2009) at  $z_s = 2.24$  and SDSS J2343–0050 (ULAS J234311.93-005034.0; Jackson et al. 2008) with  $i = 20.10$  at  $z_s = 0.787$ . The second of these lensed quasars was previously discovered by Jackson et al. (2009) from the UKIDSS (UKIRT Infrared Deep Sky Survey; Lawrence et al. 2007) and SDSS. There are two lenses among the DR5 quasars known from other surveys, SDSS J1004+1229 (J1004+1229; see CASTLES webpage) and SDSS J0820+0812 (ULAS J082016.1+081216; Jackson et al. 2008). They are not identified in our selection algorithm because of the large magnitude differences  $|\Delta I| > 1.25$  between the two images. Together with 11 lenses that are derived from the DR3 sample but do not satisfy our selection criteria (Surdej et al. 1987; Bade et al. 1997; Morgan et al. 2001; Reimers et al. 2002; Winn et al. 2002; Johnston et al. 2003; Morgan et al. 2003; Pindor et al. 2004; Inada et al. 2007, 2008; Oguri et al. 2008b), we present a list of 17 additional lensed quasars in the entire DR5 quasar sample in Table 5. We note that SDSS J1322+1052 and SDSS J1349+1227 (Section 5.1) are included in this additional sample. The details of all lensed quasars in the additional sample are also given in the references cited in Table 5.

## 6. SUMMARY

We have completed our systematic lensed quasar search in the SDSS-I quasar sample presented in the DR5 quasar catalog (Schneider et al. 2007). With follow-up observations for 136 lens candidates, we found ten lensed quasars beyond our DR3 sample. Eight of them, including one previously known, are catalogued in our complete statistical lensed quasar sample within specified separation ranges and magnitude differences. These conditions minimize our selection bias for lensed systems. Combining with the result from DR3, we present a complete sample of 19 lensed quasars selected from 36,278 quasars, where three of them have quadruple-image configurations. We then updated cosmological constraints obtained in Paper III, and obtained results consistent with other cosmological observations (e.g., Komatsu et al. 2009).

In addition to the 19 lensed quasars in our complete sample, the DR5 quasar catalog contains at least 17 additional lenses. Two were discovered among the 136 lens candidates considered here but excluded from our complete lens sample, and two were discovered from quasars outside the source sample of the 36,278 quasars. The remaining 13 lenses include two previously known lenses and 11 lenses from the DR3 sample (Paper II). These numbers may be compared with those of the CLASS, which contains 13 lenses in their statistical sample with well defined criteria and 22 lenses in total among 8958 quasars.

In this paper, we have also report the discovery of 7 binary quasars with nearly identical redshifts, as well as 8 projected quasar pairs. These quasar pairs are a useful addition to the studies of the small-scale correlation function and interaction of quasars (Hennawi et al. 2006a; Myers et al. 2008; Green et al. 2010) and the spatial distribution of absorbers (Bowen et al. 2006; Hennawi et al. 2006b; Tytler et al. 2009).

The quasar sample used in the present work is constructed from the full SDSS-I data set, and hence the work represents the completion of our statistical lens sample in the SDSS-I. We plan to continue our lens survey further to construct the SQLS lens sample from the SDSS-II, using the DR7 quasar catalog (Schneider et al. 2010). More detailed analysis of cosmological constraints will be presented elsewhere.

N. I. acknowledges support from the Special Postdoctoral Researcher Program of RIKEN, the RIKEN DRI Research Grant, and MEXT KAKENHI 21740151. This work was supported in part by Department of Energy contract DE-AC02-76SF00515. I. K. acknowledges support by Grant-in-Aid for JSPS Fellows and Grant-in-Aid for Scientific Research on Priority Areas No. 467. M-S. S. and M. A. S. acknowledge the support of NSF grant AST-0707266. A. C. is supported by grants from MIDEPLAN (ICM/P06-045-F) and CONICYT (FON-

DAP 15010003 and PFB 06). J. R. G acknowledges the support of NSF grant AST-0406713. C. S. K. is supported by NSF grant AST-0708082.

Use of the UH 2.2-m telescope and the UKIRT 3.8-m telescope for the observations is supported by the National Astronomical Observatory of Japan (NAOJ). This work is also based in part on observations obtained with the MDM 2.4m Hiltner telescope, which is owned and operated by a consortium consisting of Columbia University, Dartmouth College, the University of Michigan, the Ohio State University and Ohio University. Some of the data presented herein were obtained at the W.M. Keck Observatory, which is operated as a scientific partnership among the California Institute of Technology, the University of California and the National Aeronautics and Space Administration. The Keck Observatory was made possible by the generous financial support of the W.M. Keck Foundation. Based in part on observations made with a telescope (ESO 3.6-m) at the European Southern Observatories La Silla in Chile. Based in part on observations obtained with the Apache Point Observatory 3.5-meter telescope, which is owned and operated by the Astrophysical Research Consortium. Based on data collected at Subaru Telescope, which is operated by the National Astronomical Observatory of Japan, and obtained from the SMOKA, which is operated by the Astronomy Data Center, National Astronomical Observatory of Japan. The WB 6.5-m telescope is the first telescope of the Magellan Project; a collaboration between the Observatories of the Carnegie Institution of Washington, University of Arizona, Harvard University, University of Michigan, and Massachusetts Institute of Technology to construct two 6.5 Meter optical telescopes in the southern hemisphere. The WIYN Observatory is a joint facility of the University of Wisconsin-Madison, Indiana University, Yale University, and the National Optical Astronomy Observatories. Telescopio Nazionale Galileo (TNG) operated on the island of La Palma by the Fundacion Galileo Galilei of the INAF (Istituto Nazionale di Astrofisica) at the Spanish Observatorio del Roque de los Muchachos of the Instituto de Astrofisica de Canarias. Based in part on observations with Kitt Peak National Observatory, which is operated by AURA under cooperative agreement with the National Science Foundation.

Funding for the SDSS and SDSS-II was provided by the Alfred P. Sloan Foundation, the Participating Institutions, the National Science Foundation, the U.S. Department of Energy, the National Aeronautics and Space Administration, the Japanese Monbukagakusho, the Max Planck Society, and the Higher Education Funding Council for England.

The SDSS was managed by the Astrophysical Research Consortium for the Participating Institutions. The Participating Institutions were the American Museum of Natural History, Astrophysical Institute Potsdam, University of Basel, Cambridge University, Case Western Reserve University, University of Chicago, Drexel University, Fermilab, the Institute for Ad-

vanced Study, the Japan Participation Group, Johns Hopkins University, the Joint Institute for Nuclear Astrophysics, the Kavli Institute for Particle Astrophysics and Cosmology, the Korean Scientist Group, the Chinese Academy of Sciences (LAMOST), Los Alamos National Laboratory, the Max-Planck-Institute for Astronomy (MPIA), the Max-Planck-Institute for Astrophysics (MPA), New Mexico State University, Ohio State University, University of Pittsburgh, University of Portsmouth, Princeton University, the United States Naval Observatory, and the University of Washington.

## REFERENCES

- Abazajian, K., et al. 2003, *AJ*, 126, 2081
- Abazajian, K., et al. 2004, *AJ*, 128, 502
- Abazajian, K., et al. 2005, *AJ*, 129, 1755
- Abazajian, K., et al. 2009, *ApJS*, 182, 543
- Adelman-McCarthy, J. K., et al. 2006, *ApJS*, 162, 38
- Adelman-McCarthy, J. K., et al. 2007, *ApJS*, 172, 634
- Baba, H., et al. 2002, *ADASS XI*, eds. D. A. Bohlender, D. Durand, & T. H. Handley, *ASP Conference Series*, 281, 298
- Bade, N., Siebert, J., Lopez, S., Voges, W., & Reimers, D. 1997, *A&A*, 317, L13
- Becker, R. H., White, R. L., & Helfand, D. J. 1995, *ApJ*, 450, 559
- Blandford, R. D. & Kochanek, C. S. 1987, *Gravitational Lenses, Dark Matter in the Universe*, Bachall, J., Piran, T. & Weinberg, S., eds. (World Scientific: Singapore), 103
- Blanton, M. R., Lin, H., Lupton, R. H., Maley, F. M., Young, N., Zehavi, I., & Loveday, J. 2003, *AJ*, 125, 2276
- Bolton, A. S., Burles, S., Koopmans, L. V. E., Treu, T., & Moustakas, L. A. 2006, *ApJ*, 638, 703
- Bolton, A. S., Burles, S., Koopmans, L. V. E., Treu, T., Gavazzi, R., Moustakas, L. A., Wayth, R., & Schlegel, D. J. 2008, *ApJ*, 682, 964
- Bowen, D. V., et al. 2006, *ApJ*, 645, L105

- Browne, I. W. A., et al. 2003, MNRAS, 341, 13
- Cabanac, R. A., et al. 2007, A&A, 461, 813
- Chae, K.-H., Mao, S., & Kang, X. 2006, MNRAS, 373, 1369
- Chae, K.-H. 2010, MNRAS, 402, 2031
- Choi, Y.-Y., Park, C., & Vogeley, M. S. 2007, ApJ, 658, 884
- Eigenbrod, A., Courbin, F., Dye, S., Meylan, G., Sluse, D., Vuissoz, C., & Magain, P. 2006, A&A, 451, 747
- Eigenbrod, A., Courbin, F., Meylan, G., Vuissoz, C., & Magain, P. 2006, A&A, 451, 759
- Eigenbrod, A., Courbin, F., & Meylan, G. 2007, A&A, 465, 51
- Eisenstein, D. J., et al. 2005, ApJ, 633, 560
- Faure, C., et al. 2008, ApJS, 176, 19
- Féron, C., Hjorth, J., McKean, J. P., & Samsing, J. 2009, ApJ, 696, 1319
- Fukugita, M., Futamase, T., & Kasai, M. 1990, MNRAS, 246, 24P
- Fukugita, M., Ichikawa, T., Gunn, J. E., Doi, M., Shimasaku, K., & Schneider, D. P. 1996, AJ, 111, 1748
- Green, P. J., Myers, A. D., Barkhouse, W. A., Mulchaey, J. S., Bennert, V. N., Cox, T. J., & Aldcroft, T. L. 2010, ApJ, 710, 1578
- Gregg, M. D., Lacy, M., White, R. L., Glikman, E., Helfand, D., Becker, R. H., & Brotherton, M. S. 2002, ApJ, 564, 133
- Gunn, J. E., et al. 2006, AJ, 131, 2332
- Gunn, J. E., et al. 1998, AJ, 116, 3040
- Hall, P. B., Richards, G. T., York, D. G., Keeton, C. R., Bowen, D. V., Schneider, D. P., Schlegel, D. J., & Brinkmann, J. 2002, ApJ, 575, L51
- Hennawi, J. F., et al. 2006a, AJ, 131, 1
- Hennawi, J. F., et al. 2006b, ApJ, 651, 61
- Hogg, D. W., Finkbeiner, D. P., Schlegel, D. J., & Gunn, J. E. 2001, AJ, 122, 2129



- Inada, N., et al. 2003a, *AJ*, 126, 666
- Inada, N., et al. 2003b, *Nature*, 426, 810
- Inada, N., et al. 2005, *AJ*, 130, 1967
- Inada, N., et al. 2006, *AJ*, 131, 1934
- Inada, N., et al. 2007, *AJ*, 133, 206
- Inada, N., et al. 2008, *AJ*, 135, 496 (Paper II)
- Inada, N., et al. 2009, *AJ*, 137, 4118
- Ivezić, Ž., et al. 2004, *AN*, 325, 583
- Jackson, N., Ofek, E. O., Oguri, M. 2008, *MNRAS*, 387, 741
- Jackson, N., Ofek, E. O., Oguri, M. 2009, *MNRAS*, accepted
- Johnston, D. E., et al. 2003, *AJ*, 126, 2281
- Kayo, I. et al. 2009, *AJ*, in press.
- Kneib, J.-P., Cohen, J. G., & Hjorth, J. 2000, *ApJ*, 544, L35
- Kochanek, C. S., Falco, E. E, & Muñoz, J. A. 1999, *ApJ*, 510, 590
- Kochanek, C. S., Schneider, P., & Wambsganss, J. 2006, Part 2 of Gravitational Lensing: Strong, Weak & Micro, Proceedings of the 33rd Saas-Fee Advanced Course, G. Meylan, P. Jetzer & P. North, eds. (Springer-Verlag: Berlin), 91
- Komatsu, E., et al. 2009, *ApJS*, 180, 330
- Kubo, J. M., Allam, S. S., Annis, J., Buckley-Geer, E. J., Diehl, H. T., Kubik, D., Lin, H., & Tucker, D. 2009, *ApJ*, 696, L61
- Kundic, T., Cohen, J. G., Blandford, R. D., & Lubin, L. M. 1997, *AJ*, 114, 507
- Lacy, M., Gregg, M., Becker, R. H., White, R. L., Glikman, E., Helfand, D., & Winn, J. N. 2002, *AJ*, 123, 2925
- Lawrence, A., et al. 2007, *MNRAS*, 379, 1599
- Lubin, L. M., Fassnacht, C. D., Readhead, A. C. S., Blandford, R. D., & Kundić, T. 2000, *AJ*, 119, 451

- Lupton, R., Gunn, J. E., Ivezić, Z., Knapp, G. R., Kent, S., & Yasuda, N. 2001, in ASP Conf. Ser. 238, *Astronomical Data Analysis Software and Systems X*, ed. F. R. Harnden, Jr., F. A. Primini, and H. E. Payne (San Francisco: Astr. Soc. Pac.), p. 269
- Maoz, D., et al. 1993, *ApJ*, 409, 28
- Marshall, P. J., Hogg, D. W., Moustakas, L. A., Fassnacht, C. D., Bradač, M., Schrabback, T., & Blandford, R. D. 2009, *ApJ*, 694, 924
- Mitchell, J. L., Keeton, C. R., Frieman, J. A., & Sheth, R. K. 2005, *ApJ*, 622, 81
- Morgan, N. D., Becker, R. H., Gregg, M. D., Schechter, P. L., & White, R. L. 2001, *AJ*, 121, 611
- Morgan, N. D., Snyder, J. A., & Reens, L. H. 2003, *AJ*, 126, 2145
- Morokuma, T., et al. 2007, *AJ*, 133, 214
- Muñoz, J. A., Falco, E. E., Kochanek, C. S., McLeod, B. A., & Mediavilla, E. 2003, *ApJ*, 605, 614
- Myers, S. T., et al. 2003, *MNRAS*, 341, 1
- Myers, A. D., Richards, G. T., Brunner, R. J., Schneider, D. P., Strand, N. E., Hall, P. B., Blomquist, J. A., & York, D. G. 2008, *ApJ*, 678, 635
- Ofek, E. O., Oguri, M., Jackson, N., Inada, N., & Kayo, I. 2007, *MNRAS*, 382, 412
- Oguri, M., et al. 2004, *PASJ*, 56, 399
- Oguri, M., et al. 2005b, *ApJ*, 622, 106
- Oguri, M., et al. 2006, *AJ*, 132, 999 (Paper I)
- Oguri, M. 2007a, *ApJ*, 660, 1
- Oguri, M. 2007b, *New Journal of Physics*, 9, 442
- Oguri, M., et al. 2008a, *AJ*, 135, 512 (Paper III)
- Oguri, M., et al. 2008b, *AJ*, 135, 520
- Oscos, A., Serra-Ricart, M., Mediavilla, E., Buitrago, J., & Goicoechea, L. J. 1997, *ApJ*, 491, L7

- Padmanabhan, N., et al. 2008, *ApJ*, 674, 1217
- Peng, C. Y., Ho, L. C., Impey, C. D., & Rix, H.-W. 2002, *AJ*, 124, 266
- Pier, J. R., Munn, J. A., Hindsley, R. B., Hennessy, G. S., Kent, S. M., Lupton, R. H., & Ivezić, Ž. 2003, *AJ*, 125, 1559
- Pindor, B., et al. 2004, *AJ*, 127, 1318
- Pindor, B., et al. 2006, *AJ*, 131, 41
- Poggianti, B. M. 1997, *A&A*, 122, 399
- Reimers, D., Hagen, H.-J., Baade, R., Lopez, S., & Tytler, D. 2002, *A&A*, 382, L26
- Richards, G. T., et al. 2002, *AJ*, 123, 2945
- Richards, G. T., et al. 2005, *MNRAS*, 360, 839
- Rusin, D., & Tegmark, M. 2001, *ApJ*, 553, 709
- Rusin, D. 2002, *ApJ*, 572, 705
- Rusin, D, et al. 2003, *ApJ*, 587, 143
- Ryan, R. E., Jr., Cohen, S. H., Windhorst, R. A., Keeton, C. R., & Veach, T. J. 2008, *ApJ*, 688, 43
- Schlegel, D. J., Finkbeiner, D. P., & Davis, M. 1998, *ApJ*, 500, 525
- Schneider, D. P., et al. 2005, *AJ*, 130, 367
- Schneider, D. P., et al. 2007, *AJ*, 134, 102
- Schneider, D. P., et al. 2010, *AJ*, 139, 2360
- Schneider, P., Ehlers, J., & Falco, E. E. 1992, *Gravitational Lenses*, (Berlin: Springer-Verlag)
- Smith, J. A., et al. 2002, *AJ*, 123, 2121
- Stoughton, C., et al. 2002, *AJ*, 123, 485
- Surdej, J., Swings, J.-P., Magain, P., Courvoisier, T. J.-L., & Borgeest, U. 1987, *Nature*, 329, 695
- Tegmark, M., et al. 2006, *Phys. Rev. D*, 74, 123507

Tucker, D. L., et al. 2006, AN, 327, 821

Turner, E. L., Ostriker, J. P., & Gott, J. R., III 1984, ApJ, 284, 1

Turner, E. L. 1990, ApJ, 365, L43

Tytler, D., et al. 2009, MNRAS, 392, 1539

Walsh, D., Carswell, R. F., & Weymann, R. J. 1979, Nature, 279, 381

Weymann, R. J., et al. 1980, Nature, 285, 641

Winn, J. N., Lovell, J. E. J., Chen, H.-W., Fletcher, A. B., Hewitt, J. N., Patnaik, A. R., & Schechter, P. L. 2002, ApJ, 564, 143

York, D. G., et al. 2000, AJ, 120, 1579

Young, P., Gunn, J. E., Oke, J. B., Westphal, J. A., & Kristian, J. ApJ, 241, 507

Table 1. NUMBERS OF CANDIDATES

	Number
SDSS DR5 spectroscopically confirmed quasars	77,429
DR5 quasars <i>not</i> passing the criteria ( $0.6 < z < 2.2$ , $i < 19.1$ , and $\text{PSF\_WIDTH} < 1''.8$ )	–41,142
Source quasar sample	36,287
DR3 quasars (checked in Paper II)	–22,651 <sup>a</sup>
Source quasars to complete the DR5 statistical lens sample	13,636
Initial morphologically selected candidates (using <code>star_L</code> in <i>ugri</i> )	401
Rejected by GALFIT fitting	–348
Rejected by visual inspection	–3
Final morphologically selected candidates for follow-up	50
Initial color selected candidates	140
Rejected by FIRST image check	–5
Rejected by visual inspection	–6
Rejected by searching for possible lens objects	–41
Final color selected candidates for follow-up	88
Final total (morphological+color) candidates for follow-up	136 <sup>b</sup>

<sup>a</sup>The number of the source quasars in the paper II is 22,683, but 32 DR3 quasars do not meet the criteria in the DR5 catalog.

<sup>b</sup>Two candidates are selected by both the morphological and color selection algorithms. They are listed in Table 2 as morphologically selected candidates.

Table 2. Morphologically Selected Candidates

Object	redshift <sup>a</sup>	$i^b$	$\theta_{\text{SDSS}}^c$	$ \Delta i ^c$	image <sup>d</sup>	spec <sup>d</sup>	comment	Ref.
SDSS J024519.65−005113.0	1.545	18.78	1.12	1.24	UF( $K$ )	...	QSO+galaxy	...
SDSS J030556.81+005701.7	0.893	19.00	2.09	1.46	UF( $K$ )	...	QSO+galaxy	...
SDSS J074653.03+440351.3	1.998	18.71	1.07	0.04	8k( $VRI$ ),RE( $r$ ),Op( $I$ )	ES	SDSS lens	1
SDSS J074942.51+171512.1	2.163	18.87	1.01	0.82	Te( $I$ )	...	no lens object	...
SDSS J080009.98+165509.4	0.708	17.97	0.79	0.03	Te( $I$ )	...	no lens object	...
SDSS J080623.70+200631.8	1.537	18.88	1.42	0.26	8k( $VRI$ ),QU( $H$ ),NR( $K'$ )	ES	SDSS lens	2
SDSS J082312.13+264415.7	1.855	18.16	1.40	1.42	Te( $I$ )	...	QSO+galaxy	...
SDSS J082341.08+241805.4	1.811	16.90	0.58	0.04	8k( $V$ )	...	single QSO	...
SDSS J083240.71+060759.3	0.808	19.04	1.58	1.92	Te( $I$ )	...	no lens object	...
SDSS J094713.15+024743.6	0.641	18.99	1.57	1.11	Te( $I$ )	...	no lens object	...
SDSS J095237.05+290834.6	1.413	18.22	4.55	1.14	Te( $I$ )	...	QSO+galaxy	...
SDSS J104901.21+121214.1	1.572	19.09	1.50	0.84	...	EF	QSO+unknown(not QSO)	...
SDSS J105545.44+462839.5	1.249	18.75	1.12	0.89	8k( $VRI$ ),FO( $RI$ ),Te( $RI$ ),NF( $H$ )	FO	SDSS lens	3
SDSS J110456.56+130711.1	1.778	18.47	1.07	1.11	Te( $I$ )	FO	QSO+star	...
SDSS J111816.95+074558.1	1.736	15.96	2.26	1.92	...	...	known lens (PG1115)	4
SDSS J112508.26+303141.3	1.960	17.62	0.43	1.17	Te( $I$ )	...	single QSO	...
SDSS J113831.39+151215.3	0.659	18.42	0.50	2.06	Te( $I$ )	...	single QSO	...
SDSS J114217.47+451447.7	1.782	18.95	3.93	0.26	...	DA	QSO+star	...
SDSS J114443.69+350539.6	0.604	18.74	0.79	1.86	Te( $I$ )	...	single QSO	...
SDSS J115619.49+460313.8	1.235	18.11	0.44	1.75	Te( $I$ )	...	single QSO	...
SDSS J115800.91+120439.4	1.615	18.57	1.84	1.24	Te( $I$ )	...	QSO+galaxy	...
SDSS J120118.92+401318.1	1.933	18.56	1.54	1.51	Te( $I$ )	...	QSO+galaxy	...
SDSS J120239.66+455429.7	1.071	18.46	0.40	0.94	Te( $I$ )	...	single QSO	...
SDSS J120348.93+325542.5	1.217	18.89	0.47	1.80	Te( $I$ )	...	single QSO	...
SDSS J120730.01+125057.6	0.752	18.20	0.54	1.08	Te( $I$ )	...	single QSO	...
SDSS J120912.45+143602.3	1.497	18.10	0.42	0.48	Te( $I$ )	...	single QSO	...
SDSS J121357.15+083202.2	0.811	18.01	0.41	0.87	Te( $I$ )	...	single QSO	...
SDSS J122848.03+151018.4	1.118	17.59	0.40	1.38	Te( $I$ )	...	single QSO	...

Table 2—Continued

Object	redshift <sup>a</sup>	$i^b$	$\theta_{\text{SDSS}}^c$	$ \Delta i ^c$	image <sup>d</sup>	spec <sup>d</sup>	comment	Ref.
SDSS J130225.24+332933.2	0.922	18.19	0.50	1.34	Te( <i>I</i> )	...	single QSO	...
SDSS J132236.41+105239.4	1.716	18.24	1.88	1.38	8k( <i>V</i> ),Te( <i>VRI</i> ),NF( <i>H</i> )	WF	SDSS lens	5
SDSS J134322.04+314827.7	0.930	18.32	0.49	0.33	Te( <i>I</i> )	...	single QSO	...
SDSS J135143.59+245248.8	1.286	19.06	1.47	1.34	Te( <i>I</i> )	...	no lens object	...
SDSS J135306.34+113804.7	1.623	16.48	1.33	0.97	8k( <i>VRI</i> ),QU( <i>H</i> ),Ma( <i>gi</i> )	ES	SDSS lens	2
SDSS J135404.14+110725.7	1.318	18.26	1.34	1.31	Te( <i>I</i> )	...	no lens object	...
SDSS J141202.70+354247.2	1.360	19.02	1.00	1.42	Te( <i>I</i> )	...	QSO+galaxy	...
SDSS J141910.20+420746.9	0.874	17.04	0.45	1.38	Te( <i>I</i> )	...	single QSO	...
SDSS J142030.50+353328.6	1.689	18.79	1.35	2.06	8k( <i>I</i> )	...	QSO+galaxy	...
SDSS J142326.96+093216.5	0.633	19.03	1.58	1.75	Te( <i>I</i> )	...	no lens object	...
SDSS J143344.39+113941.9	1.447	18.42	0.73	1.31	Te( <i>V</i> )	...	single QSO	...
SDSS J143452.44+133459.5	1.689	18.26	0.55	1.34	Te( <i>I</i> )	...	single QSO	...
SDSS J144618.91+114446.2	1.243	17.66	0.43	0.65	Te( <i>I</i> )	...	single QSO	...
SDSS J145307.06+331950.5	1.192	18.89	1.69	1.17	...	ES	QSO+star	...
SDSS J150020.24+340038.9	0.732	18.90	0.63	1.51	Te( <i>I</i> )	...	single QSO	...
SDSS J151109.85+335701.7	0.799	18.96	1.10	0.69	8k( <i>V</i> ),Te( <i>I</i> ),FO( <i>I</i> )	FO	binary QSO ( $z = 0.799, 0.799$ )	...
SDSS J152938.10+300351.1	0.641	18.36	0.44	1.99	Te( <i>I</i> )	...	single QSO	...
SDSS J153325.42+361915.5	0.681	18.90	0.42	0.87	Te( <i>I</i> )	...	single QSO	...
SDSS J155000.01+300223.6	0.657	18.68	0.45	0.48	Te( <i>V</i> )	...	single QSO	...
SDSS J155225.62+300902.0	0.750	18.85	1.25	0.57	8k( <i>VI</i> ),Op( <i>I</i> ),FO( <i>I</i> ),UF( <i>K</i> )	FO	binary QSO ( $z = 0.752, 0.752$ )	...
SDSS J165743.05+221149.1	1.780	17.88	1.17	1.20	MM( <i>z</i> ),UF( <i>K</i> )	...	QSO+galaxy	...
SDSS J221227.74+005140.5	1.773	18.88	1.76	1.55	UF( <i>K</i> )	...	no lens object	...

<sup>a</sup>Redshifts from the SDSS DR5 quasar catalog.

<sup>b</sup> $i$ -band PSF magnitudes with Galactic extinction corrections from the SDSS DR5 quasar catalog.

<sup>c</sup>Image separations ( $\theta_{\text{SDSS}}$ ) in units of arcsec and absolute  $i$ -band magnitude differences ( $|\Delta i|$ ) between the expected two components, derived

from fitting the SDSS *i*-band image of each candidate with two PSFs using GALFIT.

<sup>d</sup>Instruments (and filters) used for the follow-up observations. UF: UFTI at UKIRT, 8k: UH8k at UH88, Te: Tek2k CCD at UH88, Op: Optic CCD at UH88, QU: QUIRC at UH88, WF: WFGS2 at UH88, RE: RETROCAM at MDM 2.4m, ES: ESI at Keck, NR: NIRC at Keck, EF: EFOSC2 at ESO 3.6m, NF: NICFPS at ARC 3.5m, DA: DIS III at ARC 3.5m, FO: FOCAS at Subaru, Ma: MagIC at WB 6.5m, MM: MiniMo at WIYN.

References. — (1) Inada et al. 2007; (2) Inada et al. 2006; (3) Kayo et al. 2009; (4) Weymann et al. 1980; (5) Oguri et al. 2008b.



Table 3. Color Selected Candidates

Object	redshift <sup>a</sup>	$z^b$	$\theta_{\text{SDSS}}^c$	image <sup>d</sup>	spec <sup>d</sup>	comment	Ref.
SDSS J004018.21+005530.9	2.019	18.62					
SDSS J004018.68+005525.9	2.080	19.13	8.53	...	DA	QSO pair	1
SDSS J014917.10-002141.6	1.688	18.35					
SDSS J014917.47-002158.5	2.160	19.46	17.67	...	DA	QSO pair	1
SDSS J032029.75+000650.0	1.704	19.05					
SDSS J032030.90+000658.0	...	20.34	18.99	UF( $K$ )	...	no lens object	...
SDSS J034347.00-000706.5	1.975	18.85					
SDSS J034347.48-000658.9	...	19.30	10.49	UF( $K$ )	...	no lens object	...
SDSS J072653.68+394706.9	1.599	18.92					
SDSS J072653.66+394710.6	...	18.84	3.69	Te( $I$ )	...	no lens object	...
SDSS J074550.99+503423.1	1.737	18.98					
SDSS J074550.78+503430.3	...	19.84	7.44	Te( $I$ )	...	no lens object	...
SDSS J075403.19+193740.9	1.540	19.05					
SDSS J075403.60+193734.2	...	19.98	8.87	...	DA	QSO+star	...
SDSS J080932.70+193847.2	1.670	18.49					
SDSS J080931.82+193849.3	...	19.28	12.68	Te( $I$ )	...	no lens object	...
SDSS J081210.96+070826.2	1.862	17.65					
SDSS J081210.93+070838.7	...	16.89	12.39	Te( $I$ )	...	no lens object	...
SDSS J083228.49+563234.2	0.683	18.94					
SDSS J083228.53+563237.3	...	18.91	3.09	Te( $I$ )	DA	QSO+star	...
SDSS J084109.72+250200.2	1.227	19.06					
SDSS J084109.88+250216.0	...	20.13	15.89	Te( $I$ )	...	no lens object	...
SDSS J084359.79+073229.7	2.175	19.02					
SDSS J084359.89+073215.9	...	20.28	13.97	Te( $I$ )	...	no lens object	...
SDSS J085705.91+270149.0	1.419	19.08					
SDSS J085706.14+270147.6	...	20.06	3.36	Te( $I$ )	...	no lens object	...
SDSS J090323.94+313445.6	1.217	18.99					
SDSS J090324.19+313443.6	...	19.23	3.78	Te( $I$ )	...	no lens object	...

Table 3—Continued

Object	redshift <sup>a</sup>	$i^b$	$\theta_{\text{SDSS}}^c$	image <sup>d</sup>	spec <sup>d</sup>	comment	Ref.
SDSS J090505.55+085826.4	1.082	19.03					
SDSS J090505.51+085829.3	...	20.22	2.88	Te( <i>I</i> )	...	no lens object	...
SDSS J092722.27+343321.2	1.393	18.71					
SDSS J092721.58+343309.1	...	19.99	14.87	...	DA	not QSO	...
SDSS J093514.07+372140.7	1.798	18.34					
SDSS J093514.41+372145.1	...	18.35	5.91	...	DA	QSO+star	...
SDSS J094115.37+305810.3	1.193	19.02					
SDSS J094115.49+305808.6	...	20.24	2.39	Te( <i>I</i> )	...	QSO+galaxy	...
SDSS J094132.43+112913.1	1.535	18.57					
SDSS J094131.42+112917.3	...	18.45	15.51	...	DA	QSO+star	...
SDSS J094903.46+280021.9	1.563	18.96					
SDSS J094903.56+280023.2	...	19.69	1.72	UF( <i>K</i> )	FO	QSO+star	...
SDSS J095126.56+324601.4	1.552	18.41					
SDSS J095127.53+324549.1	1.928	19.59	17.30	...	DA	QSO pair	...
SDSS J095454.99+373419.9	1.884	18.36					
SDSS J095454.74+373419.8	1.540	19.19	3.14	...	DA	QSO pair	1
SDSS J095820.72+291901.1	1.537	18.65					
SDSS J095821.77+291855.5	...	19.60	14.75	Te( <i>I</i> )	...	no lens object	...
SDSS J101211.29+365030.7	1.678	18.81					
SDSS J101211.07+365014.3	1.678	20.01	16.60	Te( <i>I</i> ),NF( <i>H</i> )	DA	no lens object, binary QSO	...
SDSS J101753.63+414931.4	2.114	18.86					
SDSS J101752.33+414922.6	...	18.97	17.08	...	DA	QSO+star	...
SDSS J102335.90+384909.4	1.362	18.95					
SDSS J102336.00+384908.2	...	19.13	1.71	Te( <i>I</i> )	...	no lens object	...
SDSS J103149.35+371055.2	2.116	19.06					
SDSS J103150.14+371052.6	...	17.76	9.73	...	DA	QSO+star	...
SDSS J103419.11+124608.0	2.104	18.77					
SDSS J103419.16+124609.9	...	18.69	1.95	Te( <i>I</i> )	...	no lens object	...

Table 3—Continued

Object	redshift <sup>a</sup>	$i^b$	$\theta_{\text{SDSS}}^c$	image <sup>d</sup>	spec <sup>d</sup>	comment	Ref.
SDSS J104655.40+292045.7	1.139	18.94					
SDSS J104654.72+292052.3	...	19.47	11.03	Te( <i>I</i> )	...	no lens object	...
SDSS J111727.07+420003.0	1.154	19.01					
SDSS J111727.08+420000.3	...	20.25	2.78	Te( <i>I</i> )	...	no lens object	...
SDSS J112331.19+134954.5	1.352	18.99					
SDSS J112331.15+134952.9	...	19.72	1.73	Te( <i>I</i> )	FO	QSO+star	...
SDSS J112856.75+143352.2	1.533	18.37					
SDSS J112856.01+143349.4	...	18.58	11.22	Te( <i>I</i> )	...	no lens object	...
SDSS J113358.60+063625.7	1.570	17.97					
SDSS J113358.01+063630.2	...	19.02	9.90	Te( <i>I</i> )	...	no lens object	...
SDSS J120450.54+442835.8	1.142	18.79					
SDSS J120450.78+442834.2	1.814	19.20	3.06	...	DA	QSO pair	1
SDSS J120629.64+433217.5	1.790	18.47					
SDSS J120629.65+433220.6	1.790	19.16	3.04	8k( <i>VRI</i> )	DA	SDSS lens	2
SDSS J121646.05+352941.5	2.012	19.08					
SDSS J121645.93+352941.6	2.012	19.86	1.45	Te( <i>VRI</i> ),NF( <i>H</i> )	WF	SDSS lens	3
SDSS J121653.10+350503.7	1.854	18.52					
SDSS J121654.53+350510.8	1.800	19.33	18.82	...	DA	QSO pair	...
SDSS J122109.50+364732.2	1.859	18.92					
SDSS J122109.47+364739.0	0.470	19.87	6.76	...	DA	QSO pair	...
SDSS J122332.63+412939.2	0.804	18.72					
SDSS J122334.17+412945.6	...	18.77	18.36	...	DA	not QSO	...
SDSS J123140.73+395722.9	1.572	18.98					
SDSS J123139.73+395721.7	...	19.56	11.63	...	DA	QSO+star	...
SDSS J123449.46+084320.2	1.830	18.86					
SDSS J123448.88+084303.9	...	19.51	18.49	...	DA	QSO+star	...
SDSS J123823.37+463439.1	1.411	19.08					
SDSS J123821.84+463445.8	1.457	19.97	17.15	...	DA	QSO pair	...

Table 3—Continued

Object	redshift <sup>a</sup>	$i^b$	$\theta_{\text{SDSS}}^c$	image <sup>d</sup>	spec <sup>d</sup>	comment	Ref.
SDSS J125104.28+151144.9	2.075	18.60					
SDSS J125103.79+151159.8	...	19.24	16.52	...	DA	not QSO	...
SDSS J131019.76+401724.2	2.054	18.81					
SDSS J131019.52+401713.9	...	20.10	10.75	...	DA	QSO+star	...
SDSS J131339.98+515128.3	1.875	17.72					
SDSS J131340.02+515129.4	1.875	17.96	1.05	Te( <i>VRI</i> )	LR	SDSS lens	4
SDSS J131403.48+415203.9	1.845	18.45					
SDSS J131403.33+415203.7	...	19.37	1.80	Te( <i>I</i> )	...	no lens object	...
SDSS J132405.28+282333.5	0.904	18.48					
SDSS J132405.19+282331.9	...	19.69	2.03	Te( <i>I</i> )	...	no lens object	...
SDSS J133615.14+285911.8	1.423	18.89					
SDSS J133614.88+285859.5	...	19.03	12.83	WF( <i>i</i> )	...	no lens object	...
SDSS J134150.74+283207.9	1.376	18.71					
SDSS J134150.49+283148.1	...	19.99	20.07	SC( <i>I</i> ) <sup>e</sup>	...	no lens object	...
SDSS J134533.26+113045.2	1.355	18.75					
SDSS J134532.93+113036.8	...	19.72	9.77	...	DA	QSO+star	...
SDSS J134929.84+122706.9	1.722	17.46					
SDSS J134930.01+122708.8	1.722	18.68	2.99	FO( <i>I</i> ),QU( <i>H</i> )	DA,FO	SDSS lens	1,5
SDSS J140530.91+350319.5	1.599	18.36					
SDSS J140529.53+350328.0	0.584	18.34	19.02	...	DA	QSO pair	...
SDSS J140951.68+384406.1	1.675	18.51					
SDSS J140950.88+384417.9	...	18.82	15.12	...	DA	QSO+star	...
SDSS J141348.55+475113.4	2.175	19.00					
SDSS J141348.27+475112.8	...	18.55	2.98	NF( <i>H</i> )	...	no lens object	...
SDSS J141938.37+125227.0	1.929	19.04					
SDSS J141937.83+125233.7	...	20.15	10.39	WF( <i>i</i> )	...	no lens object	...
SDSS J141951.10+474350.6	1.563	18.56					
SDSS J141951.14+474357.4	...	19.28	6.76	WF( <i>i</i> )	...	no lens object	...

Table 3—Continued

Object	redshift <sup>a</sup>	$i^b$	$\theta_{\text{SDSS}}^c$	image <sup>d</sup>	spec <sup>d</sup>	comment	Ref.
SDSS J142815.63+095443.5	1.467	18.48					
SDSS J142815.71+095444.8	...	19.59	1.63	Te( <i>I</i> ),NF( <i>H</i> )	...	no lens object	...
SDSS J143307.88+342315.9	1.950	19.05					
SDSS J143308.03+342317.1	...	19.85	2.10	FO( <i>I</i> ),WF( <i>i</i> )	...	no lens object	...
SDSS J143624.30+353709.4	0.767	18.71					
SDSS J143623.21+353707.6	...	18.78	13.41	...	DA	QSO+star	...
SDSS J143715.91+101010.1	1.022	18.23					
SDSS J143715.87+101008.5	...	19.12	1.76	Te( <i>I</i> )	...	no lens object	...
SDSS J144410.84+304809.6	1.731	18.17					
SDSS J144410.13+304802.7	...	18.91	11.53	WF( <i>i</i> )	...	no lens object	...
SDSS J151823.05+295925.4	1.249	18.86					
SDSS J151823.34+295939.8	...	18.72	14.76	...	DA	QSO+star	...
SDSS J151823.43+295927.6	1.249	19.88	5.28	WF( <i>i</i> )	DA	no lens object, binary QSO	...
SDSS J152626.52+413135.5	2.096	19.02					
SDSS J152626.60+413147.6	1.100	19.44	12.06	...	DA	QSO pair	...
SDSS J153937.74+302023.6	1.644	18.67					
SDSS J153937.10+302017.0	1.650	19.73	10.63	...	DA	QSO pair	...
SDSS J154515.93+051713.0	2.134	18.95					
SDSS J154515.57+051729.0	...	18.75	16.87	...	DA	QSO+star	...
SDSS J155130.62+375421.3	1.448	18.93					
SDSS J155132.07+375410.9	...	20.09	19.97	...	DO	QSO+star	...
SDSS J155218.09+045635.2	1.567	18.20					
SDSS J155217.94+045646.8	1.567	18.62	11.69	Te( <i>I</i> )	DA	no lens object, binary QSO	...
SDSS J160127.53+091255.9	1.765	18.90					
SDSS J160127.56+091258.9	...	19.60	2.97	CI( <i>I</i> ),NF( <i>H</i> )	...	no lens object	...
SDSS J160602.81+290048.7	0.770	18.31					
SDSS J160603.02+290050.9	0.770	18.38	3.45	SP( <i>i</i> )	DA	no lens object, binary QSO	6
SDSS J160614.69+230518.0	1.206	18.89					

Table 3—Continued

Object	redshift <sup>a</sup>	$z^b$	$\theta_{\text{SDSS}}^c$	image <sup>d</sup>	spec <sup>d</sup>	comment	Ref.
SDSS J160614.80+230518.1	...	19.27	1.37	Te( $I$ ),NF( $H$ ),UF( $K$ )	WF	different SED, not QSO	...
SDSS J161055.42+354404.7	1.549	18.96					
SDSS J161056.18+354418.3	...	19.40	16.36	CI( $I$ ),WF( $i$ )	...	no lens object	...
SDSS J161526.64+264813.7	2.179	18.40					
SDSS J161526.35+264819.2	...	19.56	6.74	...	DA	QSO+star	...
SDSS J161527.21+264813.7	...	19.63	7.54	...	DA	QSO+star	...
SDSS J162919.93+231919.9	0.852	18.50					
SDSS J162919.09+231933.4	...	18.68	17.81	...	DA	QSO+star	...
SDSS J163520.04+205225.1	1.775	19.03					
SDSS J163519.51+205213.9	1.775	20.07	13.61	Te( $I$ ),CI( $I$ )	DA,DO	no lens object, different SED, binary QSO	...
SDSS J164212.07+220049.0	1.552	18.55					
SDSS J164211.45+220038.0	...	19.37	14.08	FO( $I$ )	...	no lens object	...
SDSS J164302.96+132738.2	1.526	18.88					
SDSS J164302.69+132724.5	...	19.35	14.28	CI( $I$ ),WF( $i$ )	...	no lens object	...
SDSS J164655.14+194300.8	1.951	19.02					
SDSS J164656.25+194310.5	...	19.61	18.34	WF( $i$ )	...	no lens object	...
SDSS J164723.58+203314.4	0.814	18.24					
SDSS J164723.80+203308.6	...	18.94	6.55	Te( $I$ )	...	no lens object	...
SDSS J165156.72+280036.9	0.862	18.65					
SDSS J165156.98+280036.4	...	19.72	3.38	Te( $I$ )	...	QSO+galaxy	...
SDSS J165326.37+193326.5	1.534	19.10					
SDSS J165326.23+193316.3	...	18.27	10.45	WF( $i$ )	...	no lens object	...
SDSS J165502.02+260516.5	1.892	17.64					
SDSS J165501.32+260517.5	1.881	17.77	9.55	...	...	SDSS QSO, different SED, QSO pair	...
SDSS J165609.48+250857.5	2.165	18.98					
SDSS J165608.98+250853.8	...	19.03	7.84	CI( $I$ )	DO	QSO+star	...
SDSS J170438.29+212149.3	1.438	18.80					
SDSS J170438.69+212202.1	...	19.36	13.95	CI( $I$ ),WF( $i$ )	...	no lens object	...

Table 3—Continued

Object	redshift <sup>a</sup>	$i^b$	$\theta_{\text{SDSS}}^c$	image <sup>d</sup>	spec <sup>d</sup>	comment	Ref.
SDSS J170555.21+214801.8	1.249	18.93					
SDSS J170555.06+214801.7	...	19.84	2.18	UF( $K$ )	...	no lens object	...
SDSS J221953.73−010037.5	1.700	18.97					
SDSS J221953.54−010032.1	...	19.56	6.14	UF( $K$ )	...	no lens object	...
SDSS J234348.33+000202.8	1.812	19.08					
SDSS J234348.49+000203.4	...	20.14	2.38	UF( $K$ )	...	no lens object	...

Note. — Two candidates, SDSS J080623.706+200631.89 and SDSS J145307.064+331950.54, that are identified by the morphological selection algorithm as well, are listed in Table 2.

<sup>a</sup>Redshifts from the SDSS DR5 quasar catalog.

<sup>b</sup> $i$ -band PSF magnitudes with Galactic extinction corrections from the SDSS DR5 quasar catalog.

<sup>c</sup>Image separations ( $\theta_{\text{SDSS}}$ ) in units of arcsec between the two components from the SDSS imaging data.

<sup>d</sup>Instruments (and filters) used for the follow-up observations. DA: DIS III at ARC 3.5m, NF: NICFPS at ARC 3.5m, SP: SPIcam at ARC 3.5m, UF: UFTI at UKIRT, Te: Tek2k CCD at UH88, 8k: UH8k at UH88, WF: WFGS2 at UH88, QU: QUIRC at UH88, FO: FOCAS at Subaru, LR: LRIS at Keck, DO: DOLORES at TNG 3.6m, CI: CCD Imager at KPNO 2.1m.

<sup>e</sup>The data are obtained from the SMOKA (Baba et al. 2002).

References. — (1) Hennawi et al. 2006a; (2) Oguri et al. 2005; (3) Oguri et al. 2008b; (4) Ofek et al. 2007; (5) Kayo et al. 2009; (6) Myers et al. 2008.

Table 4. DR5 Statistical Sample

Object	$N_{\text{img}}$	$z_s^{\text{a}}$	$z_l^{\text{b}}$	$M_I^{\text{c}}$	$\theta_{\text{max}}^{\text{d}}$	$f_I^{\text{e}}$	Source	Comment	Ref.
SDSS J0246−0825	2	1.682	0.723	−21.9	1.04	0.34	DR3	SDSS lens	1,2,3
SDSS J0746+4403	2	2.003	0.513	−22.6	1.08	0.97	DR5	SDSS lens	4,5
SDSS J0806+2006	2	1.540	0.573	−22.3	1.40	0.76	DR5	SDSS lens	3,6
SDSS J0913+5259	2	1.377	0.830	−24.5	1.14	0.70	DR3	known lens SBS 0909+523	2,7,8
SDSS J0924+0219	4	1.524	0.394	−23.0	1.78	0.43	DR3	SDSS lens	2,9,10,11
SDSS J1001+5027	2	1.838	...	...	2.86	0.72	DR3	SDSS lens	2,12
SDSS J1001+5553	2	1.405	0.390	−24.4	6.17	0.94	DR3	known lens Q0957+561	2,13,14
SDSS J1004+4112	5	1.732	0.680	−23.9	14.62	0.23	DR3	SDSS lens	2,15
SDSS J1021+4913	2	1.720	...	...	1.14	0.40	DR3	SDSS lens	2,16
SDSS J1055+4628	2	1.249	...	...	1.19	0.33	DR5	SDSS lens	5
SDSS J1118+0745	4	1.720	0.311	−22.2	2.43	0.25	DR5	known lens PG1115+080	17,18,19
SDSS J1206+4332	2	1.789	...	...	2.90	0.74	DR5	SDSS lens	12
SDSS J1216+3529	2	2.012	...	...	1.49	0.41	DR5	SDSS lens	20
SDSS J1226−0006	2	1.121	0.517	−22.5	1.24	0.45	DR3	SDSS lens	2,21
SDSS J1313+5151	2	1.875	0.194	−21.6	1.24	0.92	DR5	SDSS lens	22
SDSS J1332+0347	2	1.445	0.191	−21.6	1.14	0.70	DR3	SDSS lens	2,24
SDSS J1335+0118	2	1.570	0.440	−22.2	1.56	0.37	DR3	SDSS lens	2,21,24
SDSS J1353+1138	2	1.629	...	...	1.41	0.40	DR5	SDSS lens	6
SDSS J1524+4409	2	1.210	0.320	−22.7	1.67	0.56	DR3	SDSS lens	2,20

<sup>a</sup>Source redshifts from follow-up observations

<sup>b</sup>Measured lens redshifts.

<sup>c</sup>Absolute magnitudes of the detected (brightest) lens galaxies. The combinations of evolution- and  $K$ -corrections are included (Poggianti 1997).

<sup>d</sup>Maximum image separations in units of arcsec.



<sup>e</sup>Flux ratios between the brightest lensed image and the farthest lensed image from the brightest image, in the *I*-band images.

References. — (1) Inada et al. 2005; (2) Paper II; (3) Eigenbrod et al. 2007; (4) Inada et al. 2007; (5) Kayo et al. 2009; (6) Inada et al. 2006; (7) Oscoz et al. 1997; (8) Lubin et al. 2000; (9) Inada et al. 2003a; (10) Ofek et al. 2007; (11) Eigenbrod et al. 2006a; (12) Oguri et al. 2005; (13) Walsh et al. 1979; (14) Young et al. 1980; (15) Inada et al. 2003b; (16) Pindor et al. 2006; (17) Weymann et al. 1980; (18) CASTLES webpage (C. S. Kochanek et al., <http://cfa-www.harvard.edu/castles/>); (19) Kundić et al. 1997; (20) Oguri et al. 2008b; (21) Eigenbrod et al. 2006b; (22) Ofek et al. 2007; (23) Morokuma et al. 2007; (24) Oguri et al. 2004.

Table 5. DR5 Additional Lensed Quasars

Object	$N_{\text{img}}$	$z_s^{\text{a}}$	$z_l^{\text{b}}$	$\theta^{\text{c}}$	$f_I^{\text{d}}$	Source	Comment	Reject <sup>e</sup>	Ref.
SDSS J0134–0931	5	2.216	0.765	0.68	0.03	DR3	known lens PMN J0134–0931	$z > 2.2, i > 19.1, \theta < 1''$	1,2,3,4
SDSS J0145–0945	2	2.719	0.491	2.23	0.15	DR3	known lens Q0142–100	$z > 2.2,  \Delta I  > 1.25$	4,5,6
SDSS J0820+0812	2	2.024	0.803	2.30	0.17	DR5	known lens ULAS J0820+0812	$ \Delta I  > 1.25$	7
SDSS J0813+2545	4	1.500	...	0.91	0.06	DR3	known lens HS 0810+2554	$\theta < 1''$	4,8
SDSS J0819+5356	2	2.237	0.294	4.04	0.23	DR5	SDSS lens	$z > 2.2,  \Delta I  > 1.25$	9
SDSS J0832+0404	2	1.115	0.659	1.98	0.22	DR3	SDSS lens	$ \Delta I  > 1.25$	4,10
SDSS J0903+5028	2	3.584	0.388	2.80	0.46	DR3	SDSS lens	$z > 2.2, i > 19.1$	4,11
SDSS J0911+0550	4	2.800	0.769	3.26	0.41	DR3	known lens RX J0911+0551	$z > 2.2$	4,12,13
SDSS J1004+1229	2	2.650	0.950	1.54	0.09	DR5	known lens J1004+1229	$z > 2.2, i > 19.1,  \Delta I  > 1.25$	14,15
SDSS J1138+0314	4	2.442	0.445	1.44	0.35	DR3	SDSS lens	$z > 2.2$	4,16
SDSS J1155+6346	2	2.890	0.176	1.83	0.50	DR3	SDSS lens	$z > 2.2$	4,17
SDSS J1322+1052	2	1.716	...	2.00	0.21	DR5	SDSS lens	$ \Delta I  > 1.25$	10
SDSS J1349+1227	2	1.722	...	3.01	0.30	DR5	SDSS lens	$ \Delta I  > 1.25$	18
SDSS J1406+6126	2	2.126	0.271	1.98	0.58	DR3	SDSS lens	$i > 19.1$	4,19
SDSS J1633+3134	2	1.511	...	0.66	0.30	DR3	known lens FBQ 1633+3134	$\theta < 1'',  \Delta I  > 1.25$	4,20
SDSS J1650+4251	2	1.547	...	1.20	0.17	DR3	SDSS lens	$ \Delta I  > 1.25$	4,21
SDSS J2343–0050	2	0.788	...	1.51	0.85	DR5	known lens ULAS J2343–0050	$i > 19.1$	22

Note. — See text for the selection of each lensed quasar.

<sup>a</sup>Source redshifts from follow-up observations

<sup>b</sup>Measured lens redshifts.

<sup>c</sup>Maximum image separations in units of arcsec.

<sup>d</sup>Flux ratios between the brightest lensed image and the farthest lensed image from the brightest image, in the  $I$ -band images.

<sup>e</sup>The reason that each lens is excluded from the statistical sample.

References. — (1) Winn et al. 2002; (2) Gregg et al. 2002; (3) Hall et al. 2002; (4) Paper II; (5) Surdej et al. 1987; (6) Eigenbrod et al. 2007; (7) Jackson et al. 2009; (8) Reimers et al. 2002; (9) Inada et al. 2009; (10) Oguri et al. 2008b; (11) Johnston et al. 2003; (12) Bade et al. 1997; (13) Kneib et al. 2000; (14) Lacy et al. 2002; (15) CASTLES webpage (C. S. Kochanek et al., <http://cfa-www.harvard.edu/castles/>). (16) Eigenbrod et al. 2006b; (17) Pindor et al. 2004; (18) Kayo et al. 2009; (19) Inada et al. 2007; (20) Morgan et al. 2001; (21) Morgan et al. 2003; (22) Jackson et al. 2008.

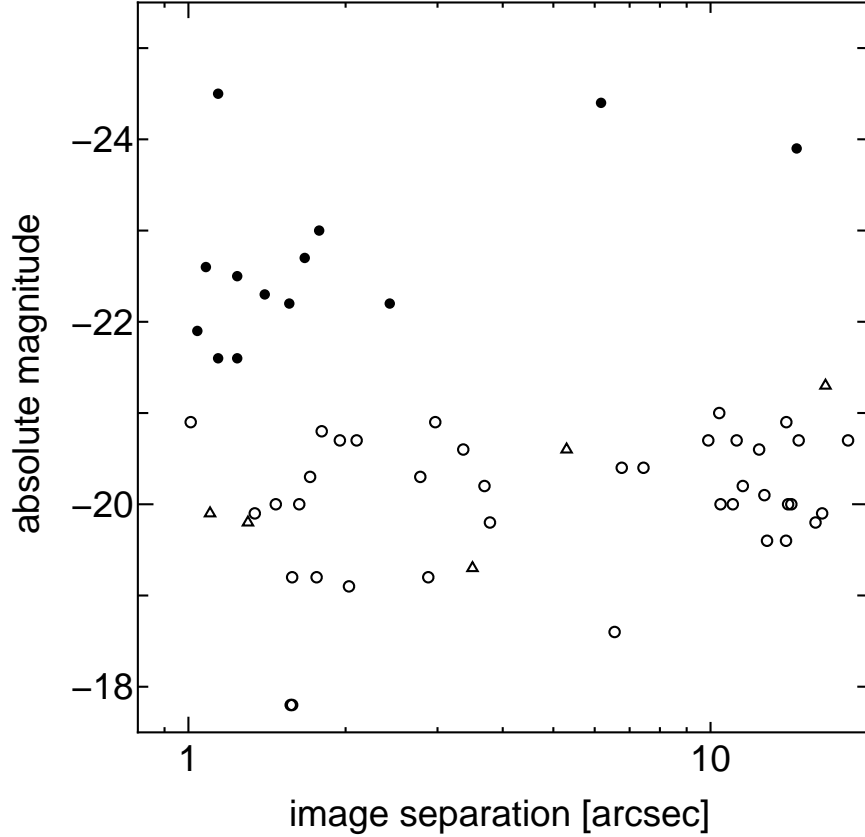


Fig. 1.— The absolute magnitudes ( $M_I$  or  $M_i$ ) of lens galaxies in our DR5 statistical sample (*filled circles*; 13 systems with known lens redshifts, listed in Table 4) are compared with detection limits of putative lens galaxies (*open circles* and *open triangles*) for our lens candidates with comments of “no lens object” and/or “binary QSO”. We concluded these lens candidates are not lensed quasars given the absence of lens galaxies to our detection limits. The absolute magnitudes for the putative lens galaxies are computed assuming  $z_l = 0.5z_s$  (*open circles*). For the five binary systems (Section 4.2), we assumed an extreme case of  $z_l = z_s$  (*open triangles*). The combinations of evolution- and  $K$ -corrections derived from the spectral model of Poggianti (1997) are included.

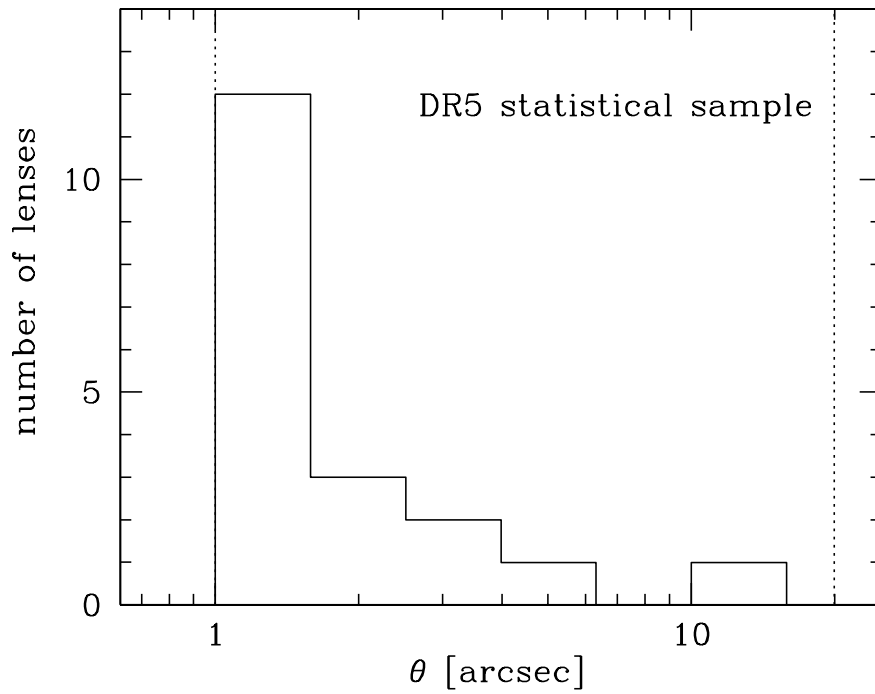


Fig. 2.— The image separation distribution of the SQLS DR5 statistical lens sample, in bins of  $\Delta \log \theta = 0.2$ . Individual lensed quasars are listed in Table 4. The dotted lines indicate upper and lower limits of the image separation for our statistical lens sample.